

Research Paper

# A COMPARISON OF CONVENTIONAL AND IRON-BASED SHAPE MEMORY ALLOYS AND THEIR POTENTIAL IN STRUCTURAL APPLICATIONS

Mihir Mishra<sup>1\*</sup> and Amin Anish Ravindra<sup>2</sup>

\*Corresponding author: **Mihir Mishra** ✉ [mihir92@gmail.com](mailto:mihir92@gmail.com)

Shape Memory Alloys (SMAs) and their applications in various fields have been known for decades. The application of SMAs in civil engineering is limited and the research is still in the pioneer phase. This paper presents the applications of SMAs in structural engineering, focused on the rehabilitation and seismic retrofit of monuments as well as their Shape Memory Effect (SME) in structures. A comparison between conventional Nitinol (NiTi) SMAs and their lower cost iron-based counterparts has also been highlighted, to determine the extent of their practical applications based on key properties that have undergone prior research. Also stated is the contrast between reinforcement grade steel and SMAs, and consequently the advantages of both, including the discussion of possible solutions to overcome their limitations. Finally, based on existing paradigms, potential regions where SMAs can be utilized to conserve cultural heritage structures have also been mentioned.

**Keywords:** Shape Memory Alloys, Damping, Structural Rehabilitation, Cultural Heritage, Structural Concrete, Civil Engineering

## INTRODUCTION

A Shape Memory Alloy (SMA) is an alloy that “remembers” its original shape, and when deformed, returns to its pre-deformed shape when heated, or upon removal of stress (Otsuka and Wayman, 1998). The prominent characteristics of SMAs, based on the type of alloy, are Superelasticity (SE), Shape Memory Effect (SME), increased damping capacity or two-way shape memory effects (Janke *et al.*, 2005). Superelasticity refers to the ability of

SMAs to undergo significant inelastic deformation under stress, and revert to their original shapes upon unloading (Dureig *et al.*, 1990). The shape memory effect, on the other hand, occurs due to the reversible phase transformation between the two crystalline structures – Martensite and Austenite (Clareda *et al.*, 2014). In the martensitic transformation, a diffusionless solid state transformation is brought about by the relative movement of atoms in an organized manner, creating a new

<sup>1</sup> Civil Engineering Department, Vellore Institute of Technology, Vellore - 632014, Tamil Nadu, India.

<sup>2</sup> Mechanical Engineering Department, Vellore Institute of Technology, Vellore - 632014, Tamil Nadu, India.

crystal structure that does not have any compositional change, but can bring about significant macroscopic deformations. This transformation is generally achieved by either quenching or mechanical deformation (Clareda *et al.*, 2014).

Austenite is stronger and stable at higher temperatures, while the weaker Martensite phase, at low temperatures, primarily due to the difference in their crystal structures, with Austenite having a body-centered cubic crystal structure whereas Martensite has an asymmetric parallelogram structure (which has 24 variations) (Song *et al.*, 2006). For this reason, the Martensite phase is weaker, being easily deformed. In contrast, Austenite, having only a single orientation, has increased resistance to external stress (Dureig *et al.*, 1990).

When applied stresses are absent, the temperature at which the martensitic (forward) transformation begins is known as  $M_s$  (martensite start) and at  $M_f$  (martensite finish), the transformation finishes. If the material is in Martensite phase ( $T < M_f$ ), then upon heating the material, the transformation can be reversed. Austenite phase formation begins at temperature  $A_s$  (austenite start) and concludes at  $A_f$  (austenite finish). The reactions with the range of temperatures have been represented in Figure 1. Due to thermal hysteresis during the transformation, the forward and reverse transformations do not occur at the same temperature (Kumar, 2008).

In 1962, Buechler and co-researchers discovered the shape memory effect in a Ni–Ti alloy (named Nitinol) (Buehler *et al.*, 1963). It was the most commonly used SMA until

1982, when the SME was observed in Fe–Mn–Si alloy and since then new iron-based SMAs have been looked into, which offer greater potential (Sato *et al.*, 1982). Two groups of iron based SMAs exist. The first group contains alloys such as Fe–Pt, Fe–Pd and Fe–Ni–Co, displaying characteristics similar to Ni–Ti thermoelastic martensitic transformations with a narrow thermal hysteresis. The latter consists of alloys like Fe–Ni–C and Fe–Mn–Si, which, despite having larger thermal hysteresis in transformation, also display SME (Maruyama, 2011).

Possible applications of SMAs in civil engineering structures were presented by authors Janke *et al.* (2005) which included passive vibration damping and energy dissipation, active vibration control, actuator applications and the utilization of the SME for tensioning applications or sensors. The damping capacity arises due to Martensite variations reorientation which exhibits SME, and also stress-induced martensitic transformation of the austenite phase, which exhibits superelasticity. The vibration suppression of civil structures can be pursued using passive control which relies on damping capacity of SMA (Song *et al.*, 2006).

The main limitation of SMAs is due to the size of the civil engineering structures and relatively high stresses, hence to be economically viable, the SMAs utilized needed to be lower in cost. Research regarding the case of damping in civil structures using iron based shape memory alloys is still in its pioneer stage. Rehabilitation of structures by using SMAs holds great promise, both in terms of damage reduction and repair cost. This paper explores the damping capacity and

other properties of Fe based SMAs and their advantages over conventional Ni-Ti alloys, as well as their potential for restoration of structures, especially cultural monuments.

## TYPES AND PROPERTIES OF SHAPE MEMORY ALLOYS

The first incidence of SME was observed in 1932 by Chang and Read in gold-cadmium (AuCd). It was only in 1962, when the same effect was seen in nickel-titanium by Buechler and his co-researchers, that the properties of SMAs were explored further (Buehler *et al.*, 1963). As mentioned earlier in the paper, this SMA, named Nitinol, was the most popular of its type. It possessed superior thermochemical and thermoelectrical properties and was readily available (Duerig *et al.*, 1963). Several properties and applications of Nitinol have been well documented. Czaderski *et al.* used NiTi wires as flexural reinforcement in a concrete beam; The stiffness and strength of the beam changed by varying the temperature in the SMA wires with electrical resistive heating (Czaderski, 2006). NiTi wires have also been used in short-fiber concrete, where the fibers were prestressed upon heating the test specimen in an oven (Moser *et al.*, 2005). In addition, recovery stresses of NiTi wires (with a specific composition and thermal treatment) were observed to be more than 200 MPa at room temperature, by Tran *et al.* (2011).

Although still holding the primary position in the industrial market, the commercial applications of NiTi are offset by the high costs of both raw materials and processing, reducing their viability. Also, their effectiveness for prestressing is restricted by their relatively

narrow thermal hysteresis, inadequate for civil engineering applications where large and stable recovery stresses are required (Lagoudas, 2008).

Alternatives in the form of iron-based SMAs are deemed more feasible for civil engineering applications due to their properties (Maruyama and Kubo, 2008). The two groups of iron-based SMAs have different applications. The first group - Fe-Pt, Fe-Pd and Fe-Ni-Co alloys, exhibit the characteristics of thermoelastic martensitic transformations similar to Ni-Ti and shows a narrow thermal hysteresis. Despite extensive studies however, pseudoelasticity at room temperature has not been reported with Fe-Pt or Fe-Pd alloys. In 2010, Tanaka *et al.* (2010) presented an Fe-29Ni-18Co-5Al-8Ta-0.01B (mass %) SMA with a recovery strain of over 13% at room temperature and high tensile strength of 1200 MPa, placing it high in the list of new materials (Ma, 2010; Ma *et al.*, 2013). It could prove to be useful for applications related to pseudoelasticity and damping capacity. Similarly, good superelastic properties have been observed at room temperature in Fe-36Mn-8Al-8.6Ni (mass %) alloy (Janke *et al.*, 2005), showing a recovery strain of over 5% and a fracture tensile strain greater than 8%. However, these alloys still need to be developed further, in order to produce large quantities for real-scale elements in the construction industry. The cost of the material would probably be high for construction standards since they need to be cast in special conditions due to their composition (Cladera *et al.*, 2014).

The second group, with Fe-Ni-C and Fe-Mn-Si, shows a larger thermal hysteresis in

transformation but still exhibits properties of SME. The primary focus, for about two decades, has been on Fe–Mn–Si SMAs, due to their low cost, good workability, good machinability and good weldability (Kajiwara, 1999), although the real applications are still limited, barring some remarkable exceptions, i.e. large size joining pipes for tunnel construction and crane rail joint bars (Maruyama *et al.*, 2011).

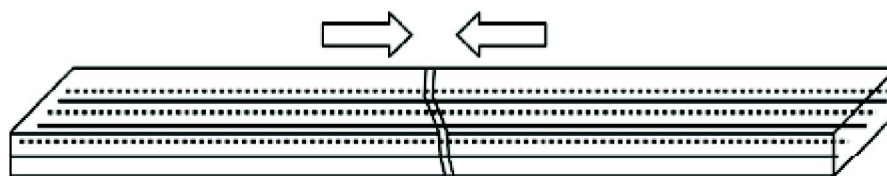
Seen from Figure 2, Fe–Mn–Si displays SME due to the stress induced martensite transformation from a parent  $\gamma$ -austenite (fcc – face-centered cubic) phase to an  $\varepsilon$ -martensite phase (hcp – hexagonal closed-packed) at low and intermediate temperature and the reverse transformation ( $\varepsilon$ - to  $\gamma$ -phase) at high temperature. Fe–Mn alloys have been known to undergo this transformation, but such an SME had not been obtained, issue being for high amounts of Mn,  $\gamma$ -austenite stabilized, the stress induced martensitic transformation was difficult to induce. On the other hand, for lower amounts of Mn, when the alloy was subjected to stress, not only  $\alpha$ -martensite but also  $\alpha'$ -martensite (bct – body-centered tetragonal) was generated, with this phase being irreversible (Figure 2c). The occurrence of  $\alpha'$ -martensite creates marked dislocations,

preventing the SME from developing (Otsuka, 1992). The addition of Si allowed the SME to occur, and this was recorded by Sato and his co-workers (Sato *et al.*, 1982). Among other elements, Chromium (Cr) was observed to be effective to some extent, suggesting that it was a suitable fourth element for the Fe–Mn–Si alloy to improve its corrosion resistance (Otsuka, 1992). The SME is reduced if the Cr amount exceeds 7%, as the brittle  $\sigma$  phase intrudes in the alloy. Ni was effective in restraining the formation of  $\sigma$  phase and thus, had to be added for increasing amounts of Cr (Otsuka, 1992).

Although in Fe–Mn–Si alloys, superelasticity cannot be observed, new research shows that some iron-based alloys such as Fe–29 Ni–18Co–5Al–8Ta–0.01B (mass %) or Fe–36Mn–8Al–8.6Ni (mass %) show super-elasticity at room temperature, but these alloys still require further development to be produced at the scale needed for civil engineering applications. As a result, they would not be cost effective (Cladera *et al.*, 2014). However, an alternative production process for the Fe–Mn–Si SMAs by mechanical alloying and subsequent sintering has been documented (Saito *et al.*, 2013). This technique, based on

**Figure 1: Schematic definition of the forward and reverse martensitic transformation temperatures [4]**

Upon electric heating, the SMA wire strands contract and reduces the crack.



powder metallurgy, involved solid state reaction among powders by high energy collisions. This may offer several advantages for manufacturing industrial products, since it allows the production of alloys in near net shape, thus minimizing the additional machining required for the final product. It produced comparable results between the mechanical properties and the shape memory effect of alloys cast using this technique, to conventional casting (Saito *et al.*, 2013).

Recovery stress is paramount for the use of iron-based SMAs as prestressing tendons in civil engineering structures. Shape recovery

properties for Fe–28Mn–6Si–5Cr SMA increase upon thermomechanical training (Maruyama *et al.*, 2011), but require additional processing, increasing the production cost and only suiting components that have simple geometries (Leinbach *et al.*, 2012; Li *et al.*, 2013). The modulus of elasticity of the Fe–28Mn–6Si–5Cr is 170 GPa (Maruyama *et al.*, 2011), higher than that reported for Ni–Ti alloys, which varies from 30 to 98 GPa in austenite to 21–52 GPa in martensite (Wen *et al.*, 2011). The recovery stresses and transformation temperatures for various Fe-Mn-Si alloys are summarized in Table 1.

**Table 1: Recovery Stresses and transformation temperatures for different Fe-Mn-Si alloys. Adapted from [4]**

S.No.	Composition in Mass %	Comments	Recovery Stress MPa	Temperature (°C)	Reference
1.	Fe-28Mn-6Si-5Cr	Without training-5-8% pre strain With training -5-8% pre strain	130 180	350 350	Maruyama <i>et al.</i> , 2011
2.	Fe-28Mn-6Si-5Cr-0.5(Nb,C)	Non pre rolled 6% pre rolled 14% pre rolled 70% pre rolled	145 255 295 200	400 400 400 400	Baruj <i>et al.</i> , 2002
3.	Fe-19Mn-5Si-8Cr-5Ni	Equal channel angular pressing and 4.5% pre strain at RT	460	500	Zhang <i>et al.</i> , 2007
4.	Fe-16Mn-5Si-10Cr-4Ni-1(V,N)	4% pre-strain at 45LC 4% pre-strain at RT	500 440	225 160	Li <i>et al.</i> , 2013
5.	Fe-15Mn-4Si-8Cr-4Ni-0.012C	Cold drawn alloy-6% pre strain at RT-Annealing temperature 650C	520	–	Wang <i>et al.</i> , 2011
6.	Fe-15Mn-4Si-8Cr-4Ni-0.12C	Cold drawn alloy-8% pre strain at RT-Annealing temperature 650C	535	–	Wang <i>et al.</i> , 2011
7.	Fe-15Mn-4Si-8Cr-4Ni-0.18C	Cold drawn alloy-4% pre strain at RT-Annealing temperature 75°C	565	–	Wang <i>et al.</i> , 2011
8.	Fe-17Mn-5Si-10Cr-4Ni-1(V,C)	4% pre-strain at RT	580	130	Leinenbach <i>et al.</i> , 2012

## COMPARISON BETWEEN NITINOL AND IRON BASED SMAS

To clarify, advantages of Nitinol include the capability of recentering and recovering more than 80% of the induced strains, high modulus of elasticity, similar behavior in tension and compression, high quality for making machined components such as bolts and high resistance to corrosion as well as fatigue. However, certain points must also be considered. Nitinol has a small area under stress-strain curve and little cyclic energy dissipation capacity.

It exhibits semibrittle and alarmless fracture with little ultimate fracture strain (less than 15%). Other problems include difficulty in welding and machining, as well as its high price (Jalaefer, 2013).

Based on the above-mentioned properties, Fe–Mn–Si alloys have shown a wider temperature transformation hysteresis and a higher elastic stiffness than Ni–Ti alloys. Also, their workability, corrosion resistance and weldability is better, in comparison. Over the years, new Fe–Mn–Si alloys with fine precipitates have been developed, allowing higher recovery stresses without, thermomechanical training (Cladera *et al.*, 2014).

Most of the research conducted for Ni–Ti alloys based on its properties and applications can be applied to iron-based shape memory alloys as well such as concrete that is prestressed by Fe–Mn–Si alloy short fibers, an idea already originally given to Ni–Ti alloys (Moser *et al.*, 2005; Shajil *et al.*, 2013), or the confinement of concrete columns, already

applied to Ni–Ti or Ni–Ti–Nb alloys (Shin, 2010; Park *et al.*, 2011). However, several such applications would demand more information about bond strength reduction of the SMA due to temperature rise. Thus, provided that in-depth future research on iron based SMAs is carried out, they seem to provide greater application opportunities.

## COMPARISON BETWEEN SMAS AND STEEL

The main advantages of structural steel as reinforcement are the capability to bear up to 35% strain before rupture, a large area under stress-strain curve or high cyclic energy dissipation capacity, gradual and alarming fracture (showing obvious deformations) and softening phase in the stress-strain curve. It is also known to exhibit similar behavior in tension and compression. Other Major factors in its favor are the simplicity of machining and welding, and especially the cost, making it viable for large scale construction.

On the offside, it has several disadvantages as well. Steel undergoes large permanent plastic strain and has a weak recentering capability. Its quality for making machined components, such as bolts, due to porosity coupled with its low resistance to fatigue, mandate the need for alternatives (Jalaefer, 2013).

Several benefits of SMAs such as Nitinol have already been discussed above in this paper. Apart from those, iron-based SMA tendons hold great promise for either reinforcing or repairing existing structures. Some of their advantages are no friction losses, no requirement for anchor heads and ducts and no space necessity for hydraulic

**Figure 2: Crystal lattices: (a)  $\gamma$ -Austenite (fcc – face-centered cubic); (b)  $\epsilon$ -Martensite (hcp – hexagonal close-packed structure); (c)  $\alpha$ -Martensite (bct – body-centered tetragonal)**

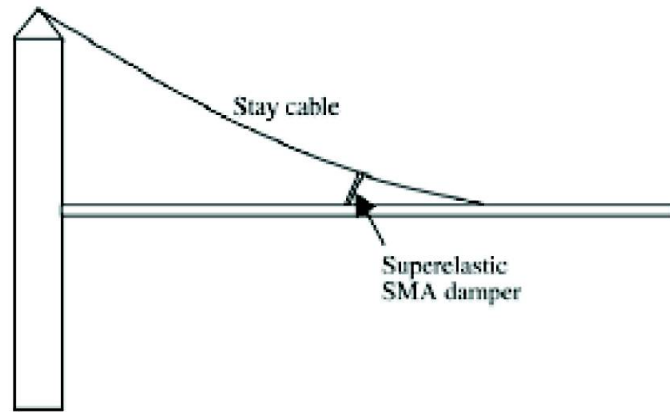


**Figure 3: Schematic of SMA damper for a stay cable bridge**

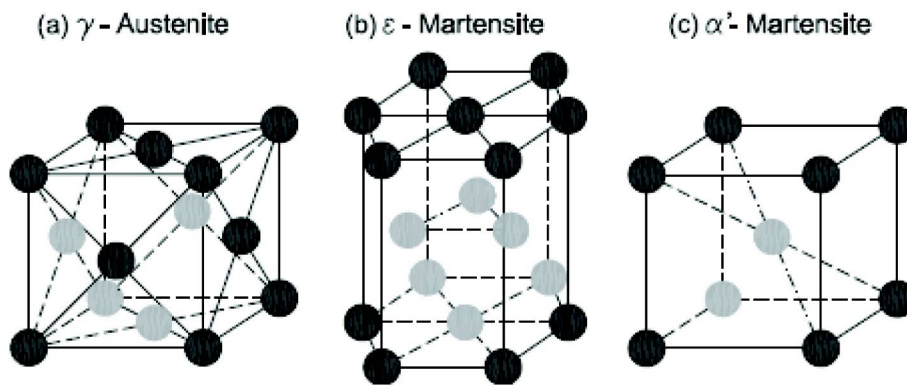


**Figure 4: Schematic of intelligent reinforced concrete specimen**

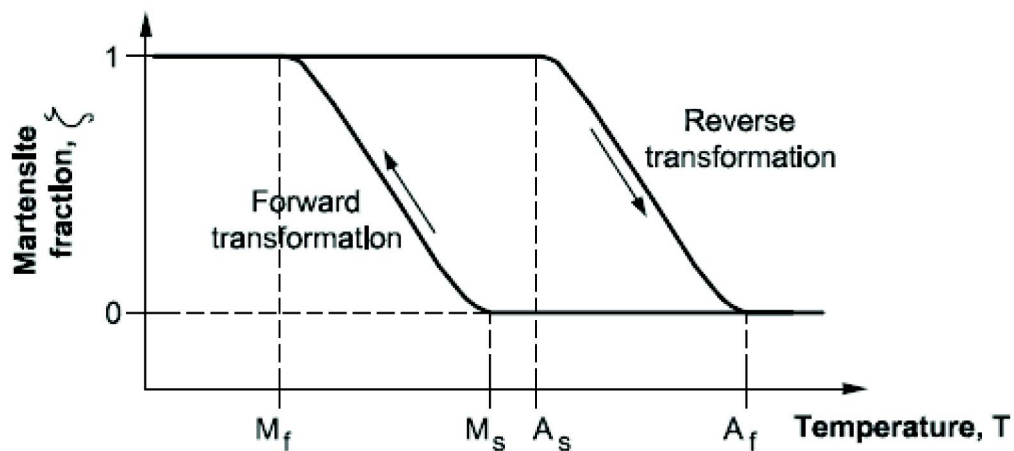
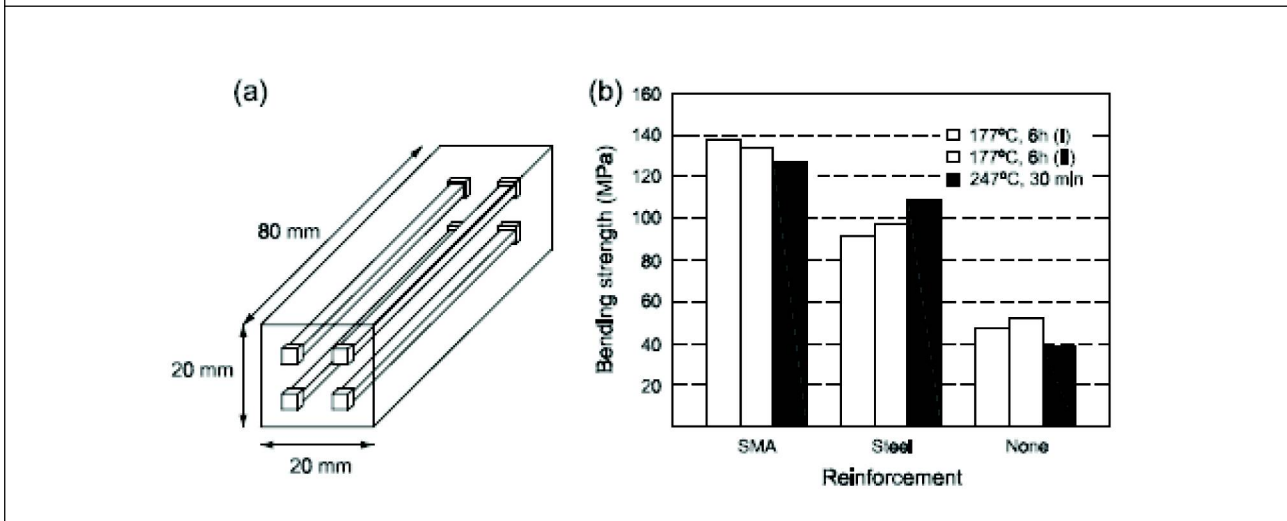


**Figure 5: Specimens tested by Sawaguchi et al. (a) bending strength of mortar specimens with SMA, steel and without reinforcement (b) [42]**



devices to apply force. New iron-based SMAs have lower costs due to the use of cheap iron (Fe) and also by melting and producing them under normal atmospheric conditions (Cladera *et al.*, 2014)

However, being highly sensitive to compositional changes, any such variations in the composition of an SMA can cause major undesirable changes in its mechanical properties. For large scale use SMAs, enforcing quality control measures would be of prime importance for proper and consistent composition which yield appropriate properties (Jalaefer, 2013). Also, Nitinol, though the most commonly used SMA, is highly expensive, and its iron based counterparts, despite being economic, still require significant research to be viable as effective replacements.

After considering all options, shape memory alloys can only be considered for use parallel to structural grade steel, by finding a middle ground where optimum benefits can be obtained, while negating maximum possible

deficiencies.

### DAMPING PROPERTIES OF SHAPE MEMORY ALLOYS

The damping capacity of SMAs come from martensite variations reorientation, which exhibit SME and stress-induced martensitic transformation of the austenite phase, which exhibit superelasticity. Three methods to suppress vibration in civil structures due to external dynamic loading exist, namely active control, semi-active control, and passive control. Passive structure control is dependent on the SMA's ability to dissipate vibration energy of structures subject to dynamic loading. Dolce and Cardone (2001) studied superelastic Nitinol wires under tension loading. The dependence of the damping capacity on temperature, loading frequency and the number of loading cycles was noted. Their results indicated that the mechanical behavior of the wires was stable within a useful range, considering seismic applications, and suggested that in order to increase efficiency of energy dissipation, the austenite wires



should be pre-tensioned (Dolce, 2001; Ip, 2000; Piedboeuf, 1998).

Liu *et al.* found that the damping capacity of a martensite Nitinol bar under tension–compression cycles increased upon increasing the strain amplitude and decreased with loading cycles, before reaching a stable minimum value (Liu *et al.*, 1999). The martensite and austenite damping of Nitinol bars, subjected to torsion was observed Dolce and Cardone. They found that the damping capacity of the martensite Nitinol bar was higher than that of the austenite Nitinol bar. However with the accumulation of residual strain, the martensite Nitinol bar could not remain at its highest value. Also observed was the martensite bar's mechanical behavior being independent of loading frequency and that of the austenite bar slightly depending on it (Dolce, 2001). It can be inferred that both martensite and austenite Nitinol bars are capable of working in a wide frequency range and are suitable for seismic protection.

## **APPLICATION OF SMAS IN CIVIL STRUCTURES**

### **Damping in Bridge Systems**

Li *et al.* used a stay-cable bridge to theoretically study the vibration mitigation of a combined cable–SMA damper system, shown in Figure 3. The SMA damped cable was made to vibrate at its first mode or at its first few modes respectively, to simulate its dynamic responses. In both cases, the authors used the results to propose the ability of superelastic SMA dampers to suppress the cable's vibration (Li *et al.*, 2004).

The utility of large martensite Nitinol bars in seismic protection devices for bridges was

studied by Casciati *et al.* (1998). To analyze the static and dynamic response of the devices to strong earthquakes a Finite Element Model (FEM) was used. The results were in agreement with the FEM analysis and verified the application of martensite Nitinol bars in energy dissipation. Hence, superelastic and martensite SMAs can be used as damping elements for bridges.

### **Application of SMAs for Structural Self-Rehabilitation**

Structural self-rehabilitation using SMAs comes under active structural control. Song and Mo proposed the concept of Intelligent Reinforced Concrete (IRC), using the actuation property of SMA wires (Song, 2003). Its intelligence is based on the ability to sense and self-rehabilitate. Figure 4 shows IRC with stranded Martensite SMA wires for post-tensioning. The electric resistance change of the shape memory alloy wires can be monitored to exhibit the strain distribution inside the concrete. Occurrence of macro-sized cracks from earthquakes can be reduced by electrically heating the SMA wire strands, causing them to contract and hence, minimize the cracks.

Small concrete blocks of dimension 13.5 in. × 6 in. × 2 in., post-tensioned by Nitinol SMA wires were fabricated and tested at University of Houston, providing convincing preliminary results (Mo *et al.*, 2004). Seven 0.015 in.-diameter SMA wires with a transformation temperature of 90° C were present in each rope. A threepoint bending test was conducted, during which upon loading, a crack measuring up to .32 in. (8 mm) opened up. Removal of the load and heating of the SMA wires reduced the crack significantly, rendering it barely

visible to the naked eye. While loading, the electrical resistance value of the SMA wire changed up to 15%. This observation allowed the monitoring of the crack opening without any additional sensors.

In Michigan, a bridge was strengthened through external post-tensioning, performed with Fe–Mn–Si–Cr SMA rebars in 2001 (Soroushian, 2001). A Fe–28Mn–6Si–5Cr alloy (manufactured by Nippon Steel Corporation) was used, capable of developing recovery stresses up to 255 MPa after heating up to 300° C. The iron-based alloy was subjected to extreme environmental temperatures, and effects on the restrained recovery stresses were examined. The results showed that the variations in stress were relatively small, and the shear crack closed to a large extent when post-tensioned with SMAs, with the load capacity of the rehabilitated beam recovered.

### Shape Memory Effect in Structural Applications

At the industrial level, crane rail fishplates have been manufactured to connect finite rail lengths for heavy duty cranes (Maruyam *et al.*, 2008), as well as steel pipe joints as a form of construction method for tunneling work (Maruyam *et al.*, 2011). In both cases, the products were manufactured by Awaji Materia Co.

A 1 mm diameter prestressed wire of Fe–27Mn–6Si–5Cr–0.05C alloy was used by Watanabe *et al.* as the reinforcement of an 80 mm long plaster prism specimen (Watanabe *et al.*, 2002). The wires were subjected to pretensile strain at room temperature (1%, 2% and 3%), and embedded into a plaster matrix.

In order to generate a compressive stress in the matrix, the specimens were heated up to 250° C. Three-point bending tests, for mechanical property characterization as well as pull-out tests were carried out, revealing that the fracture toughness of plaster could be improved by the wires. Also, as the level of pre-strain in the SMA wires was increased, the bending strength of the composite specimen increased as well.

Sawaguchi *et al.* cast small mortar prisms, reinforced with square Fe–28Mn–6Si–5Cr–1(NbC) bars (Sawaguchi *et al.*, 2006). They were embedded with SMA square bars, steel bars with the same dimensions (shown in Figure 5), or without any reinforcement, and cured for two days. Upon extraction from the mould, high-temperature curing was performed in an autoclave. The first stage of the autoclave curing at 87° C (360 K) for 24 h was carried out to increase the compressive strength of the mortar matrix. The second stage was required to pre-stress in the SMA, for which the conditions 177° C for 6 h and 247° C for 30 min, were applied. The mechanical properties of the mortar increased with the 177° C curing, but reduced for the 247° C treatment, with the exception being the prisms strengthened with steel subjected to the high temperature curing (from the results in Figure 5). It was concluded that the iron-based SMAs were usable for producing pre-stress in the mortar because the bending strength increased significantly in the specimens with the SMA compared to those either reinforced with steel or not reinforced at all. The authors further suggested that increased strength was possible if the reverse transformation temperature of the SMAs was reduced, and

as a result significant thermal damage to the mortar matrix could be avoided.

For pre-stressing concrete structures, Lee *et al.* studied the recovery stress behavior of an Fe–17Mn–5Si–10Cr–4Ni–1(V, C) alloy (Lee *et al.*, 2013) The pre-stressing effect due to SME was simulated by tests that involving pre-straining the material succeeded by heating and cooling at a constant strain. The tested SMA specimens were part of a 15 kg alloy ingot, induction melted under normal atmospheric conditions. The iron-based SMA used showed a wide hysteresis from -60 °C to 103° C obtained by a differential scanning calorimetry analysis. The highest recovery stress occurred at 400 MPa, for a pre-strain of 4% and a heating temperature of 160° C. Also, under additional loading following pre-stressing, the behavior was observed for cyclic mechanical loading and cyclic thermal loading. It was seen that the pre-stressed SMA undergoes inelastic deformation during the first cycle, reducing the recovery stress. After the first cycle though, the SMA was elastic, stress remained stable for all subsequent cycles. The study experimentally demonstrated that such a loss could be recovered completely upon reheating the SMA element.

### **Shape Memory Alloys as Seismic Retrofit**

Owing to their potential, SMAs have been used to retrofit existing or damaged structures, and protect them from further damage brought on by disasters such as earthquakes. The intensity of damage to structures is directly related to the magnitude of the earthquake on the Richter scale. Traditionally, in order to protect structures such as cultural heritage monuments from seismic behavior, localized

reinforcements such as steel bars or cables have been used, to provide an increased stability and ductility, but several cases exist where despite such provisions, structural collapse has still occurred. In fact, during a past earthquake and its resultant damage to a church, the tympana collapsed despite reinforcement through steel ties, although the remaining facades at the lower portion of the church remained standing (Doglioni, 1994).

One significant example is the Basilica of St Francis in Assisi, severely damaged during the 1999 earthquake in central Italy (Croci *et al.*, 2000; Mazzaloni, 2002). In its restoration, obtaining an adequate safety level while simultaneously maintaining its original structure was the major challenge. A connection between the tympanum and the roof was created using superelastic SMA rods so as to reduce the effect of seismic forces on it. The SMA devices exhibited different structural properties based on horizontal force levels. Under low horizontal forces, they were stiff, allowing no significant displacements, under high horizontal actions the stiffness reduced to make an allowance for controlled displacements of the masonry walls to occur, while extremely intense horizontal loads increased their stiffness to avoid structural collapse.

Another example of utilizing SMAs as seismic retrofit is in the bell tower of the San Giorgio church in Trignano, Italy, severely damaged during the 1996 earthquake (Mazzaloni, 2002; Indirli, 2000). For its rehabilitation, four vertical pre-stressing steel tie bars were inserted in the internal corners of the structure aiming to increase its flexural strength with the main aim being post-

tensioning the SMA devices so that a state of constant compression was induced. Six tight-screwing segments placed in series with four SMA devices composed of several superelastic wires formed the tie bars.

Shaking table tests on brick masonry wall mock-ups were used to simulate a part of a monument by Indirli *et al.* (2000), in order to evaluate the how effective SMAs as ties were. Test results indicated that SMAs for such purposes could be highly effective in preventing out-of-plane collapse of peripheral walls like church facades often having weak connections at floor level. The SMA ties, in comparison to traditional ties, increased resistance against out-of-plane seismic vibrations of such masonry walls by 50% (as maximum bearable peak ground acceleration without damage), due to reduced top acceleration by a minimum of 50%. Also, the tympanum structures were protected by these SMA ties, from further seismic-induced damage.

In India, several earthquakes have wreaked havoc in the past especially in the high risk zones of the Himalayan belt, Himachal Pradesh, North-East states, Maharashtra and Delhi where two tectonic plates are in constant collision. The 1905 earthquake damaged most of the monuments in Himachal Pradesh, the worst hit being Baijnath and Kangra Valley. The Kangra Fort was partially damaged while the Brajeshwari Devi temple and the belfry of Saint John's Church were totally destroyed. The rest of the church building however escaped serious damage. The most disastrous earthquake in India's recent history took place on 26 January, 2001 in Bhuj, Gujarat,

measuring 7.7 on the Richter scale. It destroyed several monuments in the region, dating back to 9th century AD. Among them are the Aina Mahal Palace (~ 200 years old), Lakhpatji's Chhatardi (AD 1752–1761) in the city of Bhuj and some of the old temples in its vicinity. The Sun Temple at Kotai (11<sup>th</sup> century AD) and the Punvareshwar Temple at Manjal (9<sup>th</sup> century AD) are among the oldest temples that were hit. While the Chhatardi collapsed completely, Aina Mahal Palace is still standing with extensive damage. These structures seem to have survived the 1819 and 1956 earthquakes, but the tremors were apparently too severe during 2001 (Sinha, 2001).

Shape Memory Alloys, however, have not been used in India in ancient monuments because they are needed at the point of foundation. Monuments are generally repaired with the top portions like the domes and roofs including walls. The foundation is usually left untouched unless the structure is completely razed. AS mentioned in this paper, significant examples such as the Basilica of St Francis in Assisi and the bell tower of the San Giorgio church in Trignano, which were severely damaged during earthquakes in Italy, have been restored using SMAs. Given these results, the potential for SMAs in this field is vast. Preservation of monuments in disaster-prone regions is possible by analyzing suitable properties of SMAs, depending on the extent of damage to the structure or the degree of bracing needed.

## RESULTS AND CONCLUSION

Some key properties of iron-based shape memory alloys as well as Nitinol, such as damping, and their applications in the

rehabilitation and seismic retrofit of civil structures have been reviewed in this paper. With the emergence of several iron-based SMAs in the past decade, the research of their properties has increased manifold. By comparison, the potential for iron-based SMAs seems to be vast, and are bound to overtake their Nitinol counterparts, since they show similar, if not better properties under the same conditions and are cost effective as well. Parallels between SMAs and reinforcement steel have also been drawn, which show that while SMAs may not be suitable as the sole reinforcement component, if used in conjunction with steel and a certain balance be achieved, it can serve to not only lower costs, but also optimize performance of said structures.

A review of the damping properties of SMAs on the basis of experiments that have been carried out, show that there is ample scope for utility in civil engineering structures, such as bridge systems. Self-rehabilitation of structures is a promising field for the near future, although further studies would be needed to assess its possibility on a larger and more commercial scale. Similarly, the shape memory effect appears to have positive results regarding the properties and strengthening of plaster and mortar systems, reinforced with SMAs, but again, research is needed to validate its feasibility with respect to actual structures.

## CONCLUSION

Past earthquakes have inflicted severe losses on India's national heritage. Given the examples on successful implementation of

SMAs to retrofit structures in Italy, which have been damaged in the past, several monuments lying in prone areas have been listed out, where such SMAs would have the same purpose. Not only has it been shown that SMAs can aid the reparation process, but structures reinforced with them have been capable of withstanding further damage as well.

Granted, for SMAs to replace conventional materials is a distant reality. However, the key topics summarized in this paper could serve as reference points to allow significant analysis of their behavior and further understanding of properties relevant to the field where they can be ideally utilized.

## REFERENCES

1. Croci G, Bonci A and Viskovic A (2000). "Use of shape memory alloy devices in the basilica of St Francis of Assisi," Proceedings of the Final Workshop of ISTECH Project - Shape Memory Alloy Devices for Seismic Protection of Cultural Heritage Structures, pp. 110–13.
2. BarujA, Kikuchi T, Kajiwara S and Shinya N (2002), "Effect of pre-deformation of austenite on shape memory properties in Fe–Mn–Si-based alloys containing Nb and C", *Mater Trans*; Vol. 43, pp. 585–8.
3. Buehler W J, Gilfrich J V and Wiley R C (1963), "Effect of low-temperature phase changes on the mechanical properties of alloys near composition TiNi", *J Appl Phys*, Vol. 34, pp. 1475–7.
4. Casciati F, Faravelli L and Petrini L (1998), "Energy dissipation in shape memory alloy devices", *Computed-Aided*

- Civil and Infrastructure Engineering*; Vol. 13, pp. 433–42.
5. Cladera A, Weber B, Leinenbach C, Czaderski C, Shahverdi M and Motavalli M (2014), “Iron based shape memory alloys for civil engineering structures: An overview”, *Construction and building materials*, Vol. 63, pp. 281-293.
  6. Czaderski C, Hahnebach B and Motavalli M (2006), “RC beam with variable stiffness and strength”, *Constr Build Mater*, Vol. 20, No. 9, pp. 824–33.
  7. Doglioni F, Moretti A and Petrini V (Eds), (1994), “Le Chiese e il Terremoto (The Churches and the Earthquake)”, Edizioni Lint, Trieste (in Italian).
  8. Dolce M and Cardone D (2001), “Mechanical behaviour of shape memory alloys for seismic application 1. Martensite and Austenite NiTi bars subjected to torsion”, *International Journal of Mechanical Sciences*; Vol. 43, pp. 2631–56.
  9. Duerig T W *et al.* (1990), *Engineering aspects of shape memory alloys*, London: Butterworth-Heinemann.
  10. Indirli M (2000), “The demo-intervention of the ISTECH Project: the bell tower of S Giorgio in Trignano (Italy),” Proceedings of the Final Workshop of ISTECH Project - Shape Memory Alloy Devices for Seismic Protection of Cultural Heritage Structures, pp. 134–146.
  11. Indirli M, Carpani B, Martelli A, Castellano M G, Infanti S, Croci G, Biritognolo M, Bonci A, Viskovic A and Viani S (2000), “Experimental tests on masonry structures provided with shape memory alloy antiseismic devices,” 12th World Conference in Earthquake Engineering, (pp. 1–8).
  12. Ip K H (2000), “Energy dissipation in shape memory alloy wire under cyclic bending”, *Smart Materials and Structures*; Vol. 9, pp. 653–9.
  13. Jalaeefar A and Asgarian B (2013), “Experimental Investigation of Mechanical Properties of Nitinol, Structural Steel, and Their Hybrid Component.” *J. Mater. Civ. Eng.*, Vol. 25, No. 10, pp. 1498–1505.
  14. Janke L, Czaderski C and Motavalli M and Ruth J (2005), “Applications of shape memory alloys in civil engineering structures – overview, limits and new ideas”, *Mater Struct*; Vol. 38, No. 279, pp. 578–92.
  15. Janke L, Czaderski C, Motavalli M and Ruth J. (2005), “Applications of shape memory alloys in civil engineering structures – overview, limits and new ideas”, *Mater Struct*; Vol. 38, pp. 578–92.
  16. Kajiwara S (1999), “Characteristic features of shape memory effect and related transformation behaviour in Fe-based alloys”, *Mater Sci Eng A*; pp. 273–275:67–88.
  17. Krstulovic-Opara N and Thiedeman P D (2000), “Active confinement of concrete members with self-stressing composites”, *ACI Struct J*; Vol. 97, pp. 297–308.
  18. Kumar P K and Lagoudas D C (2008), In: Lagoudas D C, *Shape memory alloys*.

- modeling and engineering applications*, Springer, pp. 1–51 [Chapter 1].
19. Lagoudas D C (2008), *Shape memory alloys*, Springer, pp. 435.
  20. Lee W J, Weber B, Feltrin G, Czaderski C, Motavalli M and Leinenbach C. (2013), “Stress recovery behaviour of an Fe–Mn–Si–Cr–Ni–VC shape memory alloy used for prestressing”, *Smart Mater Struct*; Vol. 22, pp. 1–9.
  21. Leinenbach C, Kramer H, Bernhard C, Eifler D (2012), “Thermo-mechanical properties of an Fe–Mn–Si–Cr–Ni–VC shape memory alloy with low transformation temperature”, *Adv Eng Mater*; Vol. 14, pp. 62–7.
  22. Li H, Liu M and Ou J P (2004), “Vibration mitigation of a stay cable with one shape memory alloy damper”, *Structural Control and Health Monitoring*; Vol. 11, pp. 1–36.
  23. Li K, Dong Z, Liu Y, and Zhang L (2013), “A newly developed Fe-based shape memory alloy suitable for smart civil engineering”, *Smart Mater Struct*: p. 22.
  24. Liu Y, Xie Z and Humbeeck J V (1999), “Cyclic deformation of NiTi shape memory alloys”, *Materials Science and Engineering*, pp. A273–275:673–8.
  25. Ma J and Karaman I (2010), “Expanding the repertoire of shape memory alloys”, *Science*; Vol. 327, pp. 1468–9.
  26. Ma J, Hornbuckle B C, Karaman I, Thompson G B, Luo Z P and Chumlyakov Y I (2013), “The effect of nanoprecipitates on the superelastic properties of FeNiCoAlTa shape memory alloy single crystals”, *Acta Mater*; Vol. 61, pp. 3445–55.
  27. Maruyama T and Kubo H (2011) In: Yamauchi K, Ohkata I, Tsuchiya K, Miyazaki S, editors, *Shape memory and superelastic alloys: technologies and applications*, Cambridge (UK): Woodhead Publishing Limited; (pp. 141–59) [Chapter 12].
  28. Maruyama T and Kubo H (2011), “Ferrous (Fe-based) shape memory alloys (SMAs): properties, processing and applications”, Woodhead Publishing Limited., pp. 141–59.
  29. Maruyama T, Kurita T, Kozaki S, Andou K, Farjami S and Kubo H. (2008), “Innovation in producing crane rail fishplate using Fe–Mn–Si–Cr based shape memory alloy”, *Mater Sci Technol*; Vol. 24: pp. 908–12.
  30. Mazzolani F M and Mandara A (2002), “Modern trends in the use of special metals for the improvement of historical and monumental structures,” *Engineering Structures*, Vol. 24, pp. 843–856.
  31. Mo Y L, Song G and Otero K (2004), “Development and testing of a proof-of-concept smart concrete structure”, In: Proceeding of smart structures technologies and earthquake engineering.
  32. Moser K, Bergamini A, Christen R and Czaderski C (2005), “Feasibility of concrete prestressed by shape memory alloy short fibers”, *Mater Struct*; Vol. 38, No. 279, pp. 593–600.
-

33. Moser K, Bergamini A, Christen R and Czaderski C (2005), "Feasibility of concrete prestressed by shape memory alloy short fibers", *Mater Struct/Mater Constr*; Vol. 38, pp. 593–600.
34. Otsuka H (1992), "Fe–Mn–Si based shape memory alloys", *Mat Res Soc Symp Proc*; Vol. 246, pp. 309–20.
35. Otsuka K and Wayman C M (1998), *Shape memory materials*, United Kingdom: Cambridge University Press.
36. Park J, Choi E, Park K and Kim H T. (2011), "Comparing the cyclic behaviour of concrete cylinders confined by shape memory alloy wire or steel jackets", *Smart Mater Struct*; Vol. 20, pp. 1–11.
37. Piedboeuf M C and Gauvin R (1998), "Damping behaviour of shape memory alloys: strain amplitude, frequency and temperature effects", *Journal of Sound and Vibration*; Vol. 214, No. 5, pp. 885–901.
38. Saito T, Kapusta C and Takasaki A (2013), "Synthesis and characterization of Fe–Mn–Si shape memory alloy by mechanical alloying and subsequent sintering", *Mater Sci Eng A*; Vol. 592, pp. 88–94.
39. Sato A, Chishima E, Soma K and Mori T (1982), "Shape memory effect in  $\gamma \rightleftharpoons \epsilon$  transformation in Fe–30Mn–1Si alloy single crystals", *Acta Metall*, Vol. 30, pp. 1177–83.
40. Sawaguchi T, Kikuchi T, Ogawa K, Kajiwara S, Ikeo Y, Kojima M, *et al.* (2006), "Development of prestressed concrete using Fe–Mn–Si-based shape memory alloys containing NbC", *Mater Trans*; Vol. 47, pp. 580–3.
41. Shajil N, Srinivasan S M and Santhanam M (2013), "Self-centering of shape memory alloy fiber reinforced cement mortar members subjected to strong cyclic loading", *Mater Struct*; Vol. 46, pp. 651–61.
42. Shin M and Andrawes B (2010), "Experimental investigation of actively confined concrete using shape memory alloys", *Eng Struct*; Vol. 32, pp. 656–64.
43. Sinha A K (2001), The Gujarat Earthquake, Asian Disaster Reduction Center.
44. Song G and Mo Y L (2003), "Increasing concrete structural survivability using smart materials", A proposal submitted to Grants to Enhance and Advance Research (GEAR), University of Houston; January.
45. Song G, Ma N and Li N M (2006), "Applications of shape memory alloys in civil structures", *Engineering Structures*, Vol. 28, pp. 1266–1274.
46. Soroushian P, Ostowari K, Nossoni A and Chowdhury H (2001), "Repair and strengthening of concrete structures through application of corrective posttensioning forces with shape memory alloys", *Transp Res Rec*: pp. 20–6.
47. Tanaka Y, Himuro Y, Kainuma R, Sutou Y, Omori T and Ishida K (2010), "Ferrous polycrystalline shape-memory alloy showing huge superelasticity", *Science*; Vol. 327, pp. 1488–90.
48. Tran H, Balandraud X and Destrebecq J F (2011), "Recovery stresses in SMA



- wires for civil engineering applications: experimental analysis and thermo-mechanical modelling”, *Materialwiss Werkstofftech*; Vol. 42, No. 5, pp. 435–43.
49. Wang C P, Wen Y H, Peng H B, Xu D Q and Li N (2011), “Factors affecting recovery stress in Fe–Mn–Si–Cr–Ni–C shape memory alloys”, *Mater Sci Eng A*; Vol. 528, pp. 1125–30.
50. Watanabe Y, Miyazaki E and Okada H (2002). Enhanced mechanical properties of Fe–Mn–Si–Cr shape memory fiber/plaster smart composite”, *Mater Trans*; Vol. 43, pp. 974–83.
51. Wen Y H, Xie W L, Li N and Li D (2007), “Remarkable difference between effects of carbon contents on recovery strain and recovery stress in Fe–Mn–Si–Cr–Ni–C alloys”, *Mater Sci Eng A*; Vol. 457, pp. 334–7.
52. Zhang W, Wen Y H, Li N and Huang S K (2007), “Remarkable improvement of recovery stress of Fe–Mn–Si shape memory alloy fabricated by equal channel angular pressing”, *Mater Sci Eng A*; pp. 454–455:19–23.